JOURNAL OF MATERIALS SCIENCE **34** (1999) 5099–5111

Studies of microstructural and mechanical properties of nylon/glass composite

Part I *The effect of thermal processing on crystallinity, transcrystallinity and crystal phases*

HELEN C. Y. CARTLEDGE
Centre for Advanced Materials Technology, Department of Mechanical and Mechatronic Engineering, University of Sydney, NSW 2006, Australia
E-mail: helen.cartledge@dsto.defence.gov.au

CAROLINE A. BAILLIE*
Department of Materials, Imperial College of Science, Technology and Medicine, Prince Consort Road, London SW7 2BP, UK

Experimental investigations were conducted to study the effect of thermal processing on microstructures of GF/PA6 composites. Different degree of crystallinity and phases of the thermoplastic matrix, and transcrystallinity of the composite interfaces were achieved at different cooling rates during the thermal processing. XRD and DSC results indicated that when the cooling rate was varied from fast to slow, the crystallinity and the ratio of the α/γ phases of nylon6 were increased in the PA6 matrix. The microscopy observations showed that columnar spherulites grew along the glass fibre in the slow cooled thin film samples associated with larger diameter of spherulite structures in the matrix. The columnar spherulite structures around the fibres may be transcrystalline layers and they disappeared with increasing cooling rate during thermal processing. It was also found that samples with large amount of voids and poor interfacial bond was found in the low holding pressure samples during the thermal processing.

1. Introduction

Because nylons are semicrystalline matrices, the properties of GF/nylon6 are influenced by the microstructure of the polymer matrix and the fibre-matrix bond. These factors, in turn, may be affected by thermal processing. Understanding the dependence of the properties of GF/nylon6 on microstructure is an important step towards the design of optimal thermal processing protocols for these thermoplastic composites.

Thermal processing is a critical aspect of thermoplastic technology. The microstructures of thermoplastic composites, such as degree of crystallinity, orientation of crystalline, the size of spherulites and the interfacial bond between fibre and matrix, depend upon many thermal processing parameters [1–4], for example, cooling rate and holding pressure. The microstructures are know to affect the mechanical properties of the composites [5]. For instance, the mechanical properties of composite materials depend on the bonding condition between the fibres and the matrix. The success of the cooperative interaction between matrix and fibre depends to a significant degree on the nature of the fibre/matrix interfacial region. In the last few years, there have been many studies of the interfacial region. These studies showed that transcrystallization and interfacial bonding strength may be altered during thermal processing of the semicrystalline thermoplastic composites [6, 7]. These microstructural changes may affect the mechanical properties of the composites [5].

Some authors considered the issue of transcrystallinity enhancing the mechanical bond between fibre and matrix [8, 9]. Lee and Porter [10] reported an approximately twofold increase in the transverse tensile strength and fracture resistance of highly transcrystalline and spherulitic specimens of continuous carbon fibre reinforced PEEK. However, as yet there has been not much measurement of such effects in bulk composite samples, and it is still debatable as to whether transcrystallinity increases or decreases the interfacial strength.

The mechanical properties of polyamides are dominated by the amount and size of the spherulites. The bulk Young's modulus and tensile strength of nylon6 increase with increasing crystallinity of the α phase [11]. The high fatigue resistance (bending mode) of nylon6 and the excellent retention of properties on repeated use have been attributed to a much narrower distribution of the long period, anti-parallel, arrangement of molecules

*Author to whom all correspondence should be addressed.

in the α crystalline form [12]. The microstructural changes and mechanical properties were improved in annealed PA6 samples were studied by Russian scientists [13]. However, these parameters are also affected by the orientation of the spherulites, which in turn is controlled by the intermolecular hydrogen bonding and chain packing in the spherulite crystals. In nylons, the spherulite crystals are formed from hydrogen-bonded sheets [14]. The crystal structures generally occur in one of four different phases: α, β, γ, or δ. This phase terminology characterises the general conformation of the polyamide chains and their mode of packing, which results from thermal processing [15].

The α and γ phases normally coexist in bulk materials. The principal differences between these two phases are the lattice parameters and the orientation of the hydrogen bonds between the NH and the C=O groups. In the α phase, the hydrogen bonds are formed in the zigzag planes and between the antiparallel chains. The hydrogen bonded molecules are stacked upon one another forming planar sheets. The molecules are in the fully extended zigzag formation and theoretically can form strain-free intermolecular hydrogen bonds [14, 16]. In the γ phase, the molecular chains twist away from the zigzag planes to form hydrogen bonds between parallel chains. This twisting of the molecules results in a slight shortening of the periodicity in the chain direction, and results in the chain repeat distance of the γ form being shorter than for the α phase [17–19].

However, the nature of thermal factors affecting the microstructures and mechanical properties is still not fully understood e.g. how the cooling rate during thermal processing affects the phases of the matrix, and transcrystallinity of the interface. Thus the objectives of this paper are to investigate the effects of the cooling rate and pressure during the thermal processing on the microstructures of the thermoplastic matrix and composite interface, and then find out how to control the microstructures in the thermal manufacturing processes.

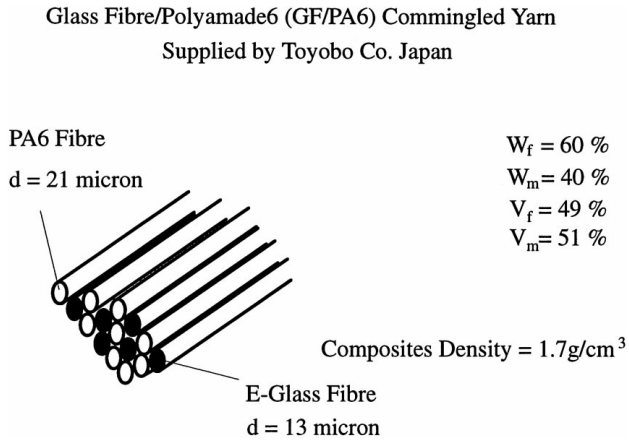

Figure 1 Schematic diagram of GF/PA6 composite system.

2. Specimen preparation

2.1. Materials system

The unidirectional commingled yarn GF/PA6 was supplied by TOYOBO Research Institute, Toyobo Co. Ltd., Japan. Fig. 1 shows the original data of the GF/PA6 commingled yarn system supplied by the manufacturer. The density of the PA6 matrix ρ_m was 1.14 g/cm^3, E-glass fibre density ρ_f was 2.58 g/cm^3 and the E-glass fibre weight fraction W_f was 60%. The E-glass fibre diameter ranged from 10 to 15 μm and PA6 fibre from 21–22 μm. A Differential Scanning Calorimetric (DSC) test was conducted to determine the thermodynamic properties of the PA6. The DSC results indicated that the melting point T_m of the crystalline PA6 was 210 °C and the glass transition temperature of the amorphous PA6 T_g was 40 °C as shown in Fig. 2.

2.2. Manufacture processes

2.2.1. Bulk samples consolidation

The GF/PA6 commingled yarn was wound unidirectionally onto the steel plate at 40 rpm giving 15 yarn per inch in the winding machine. The yarn was welded

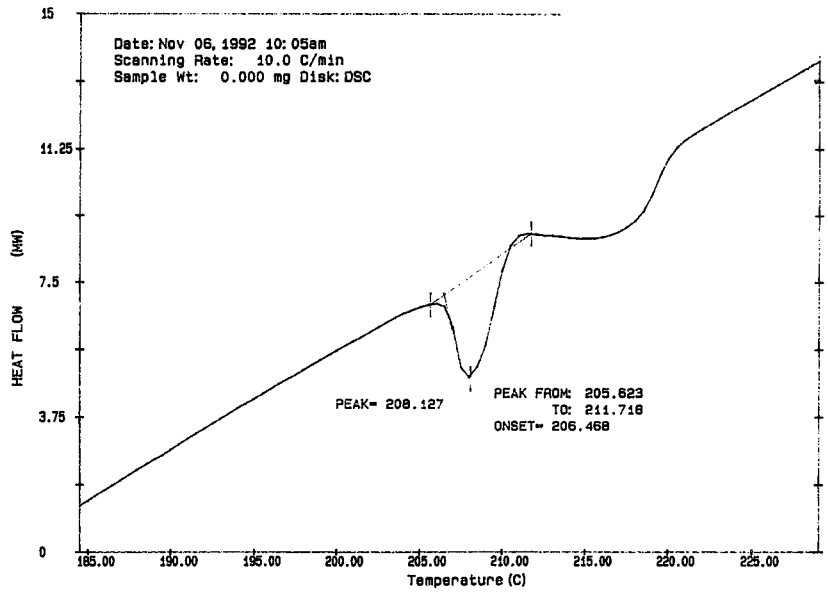

Figure 2 Differential scanning calorimetric test result of PA6 fiber before moulding.

together along a line 10 mm away from the edge of the steel plate on both sides with a 40 W soldering iron. The GF/PA6 sheets were cut off from the steel plate along the edge. Fourteen commingled yarn sheets were laid up unidirectionally in the mould. To prevent the PA6 sticking on the mould during consolation, a low surface free energy GF/PTFE cover sheet (CHEMGLAS) was inserted between the GF/PA6 composites and steel mould. The consolidation process was carried out on a hydraulic hot-press machine, Moore G748. The first stage of heating the sample above the PA6 melting temperature took approximately 10 min and pressure was applied to the top and bottom platens of the hot press machine. Once the sample reached 240 °C, the pressure was constantly kept at 1.5 MPa to squeeze out air and excess resin sealed the mould and prevented oxidation degradation of the PA6. The moulding temperature was from 235 to 240 °C and the holding time was 10 min with constant pressure through out the entire process.

To obtain the different microstructures in the composites, the moulds were cooled down at three different rates in the hydraulic press machine under 1.5 MPa pressure. A thermal measurement unit was used to record and monitor the temperature changing during the whole consolidation process.

(1) −1 °C/min, cooled down in the hot-press;
(2) −3 °C/min, cooled down with air circulated through the plates of the hot-press machine;
(3) −60 °C/min, cooled down with cold water circulated through the plates of the hot-press machine.

Fig. 3 shows the manufacturing flow chart of the GF/PA6 composite samples and Fig. 4 shows the thermal history of the composite consolidation. The final sample was of dimensions 200 × 200 × 4 mm and it was a white colour implying there were no oxidising degradation during the thermal processing.

2.2.2. Thin films consolidation

Cast thin nylon films containing single glass fibres were prepared for optical microscopy study by placing individual glass fibres with nylon fibres onto clean rectangular glass slides (1 × 25 × 75 mm) with thinner round glass slides (0.1 mm thick, 20 mm in diameter) cover on the top as Fig. 5 illustrates.

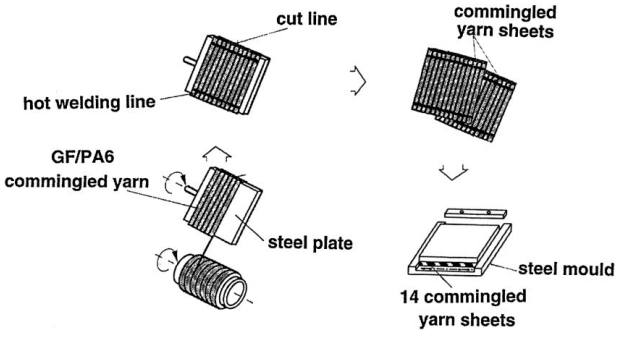

Figure 3 Manufacturing flow chart of GF/PA6 composite samples.

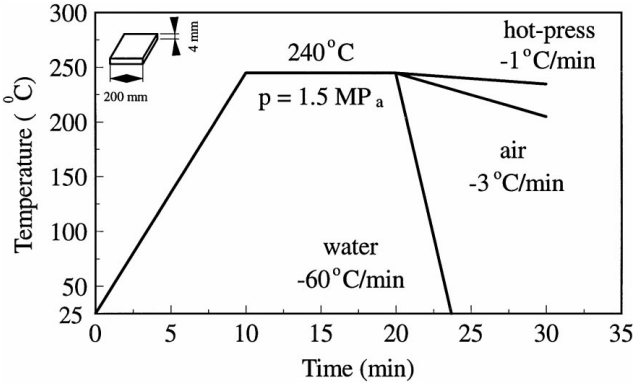

Figure 4 Thermal histories of GF/PA6 composite samples.

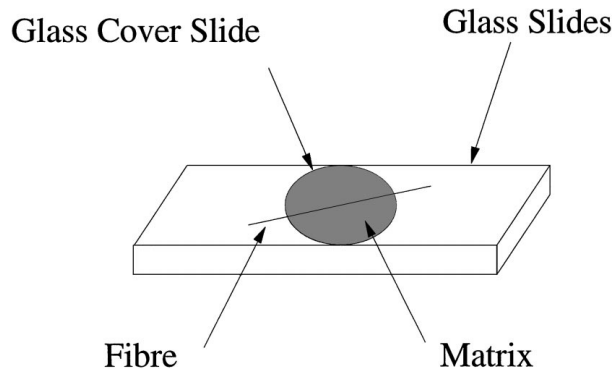

Figure 5 Thin film manufacturing procedure.

The samples were then placed in the steel mould which was used for bulk sample manufactures and heated up to melting point in the hot-press under the same pressure as the bulk samples (1.5 MPa). They were cooled down under the three different cooling processes which were outlined above. The thermal histories of these thin films samples were exactly same as that of the bulk GF/PA6 samples.

2.3. Microscopy study of consolidating processes on hot-stage

The consolidation of the thin film GF/PA6 was observed under a polarised optical microscope. The rectangular glass slide contained nylon6 fibres plus a few glass fibres, covered with a thin round glass slide was placed into the controlled hot-stage (METTLER FP 82). The hot-stage was then placed under the microscope lens, and by using the transmitted light to observe the consolidation and crystallization processes. To control the heating temperature and cooling rate, the thermal processes were conducted by the central processor METTLER FP 90.

Under the microscope it can be seen that the nylon fibres start to melt when the heating temperature reached 210 °C and then the molten nylon6 forms many big polymer bubbles. It appeared that the polymer bubbles have a difficultly flowing around and joining each other. This is may be attributed the high viscosity of the molten nylon6 matrix or high surface energy. When a pressure was applied onto the top of the glass slide, the nylon bubbles were squeezed into each other and wet

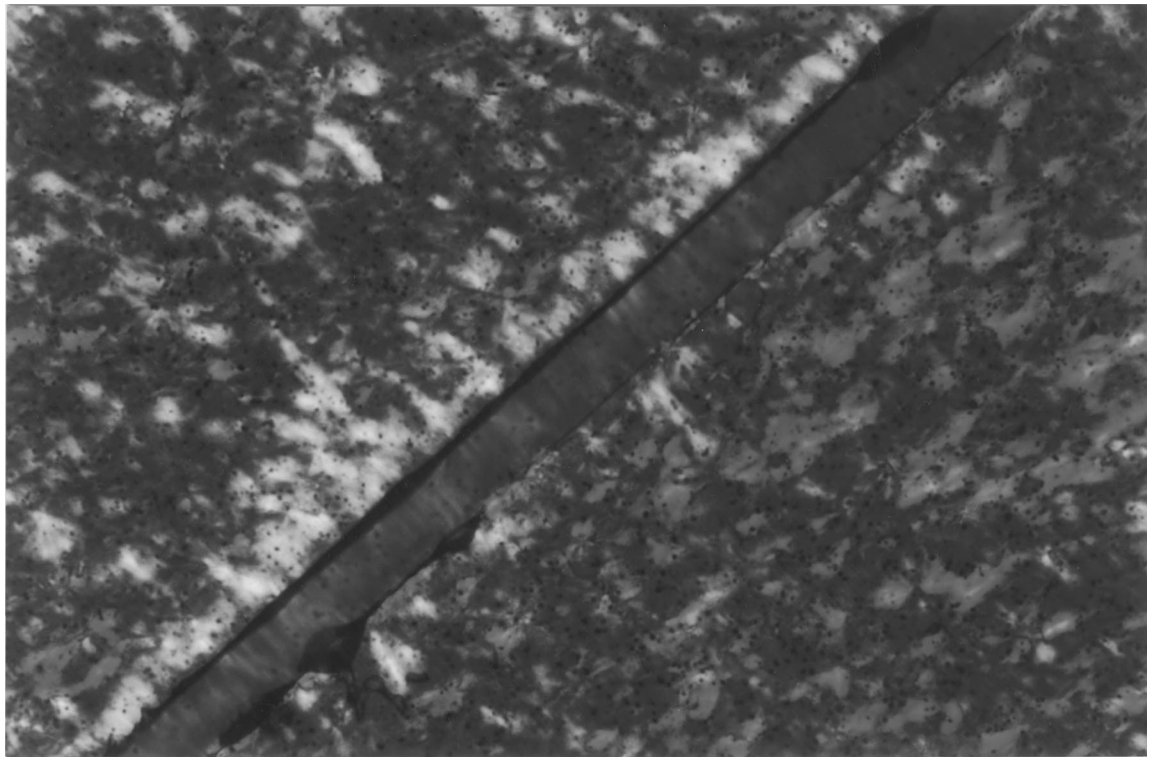

Figure 6 Polarised optical image of GF/PA6 thin film (cooling rate: $-1\,^{\circ}$C/min, holding pressure: atmosphere, magnification: $\times 625$).

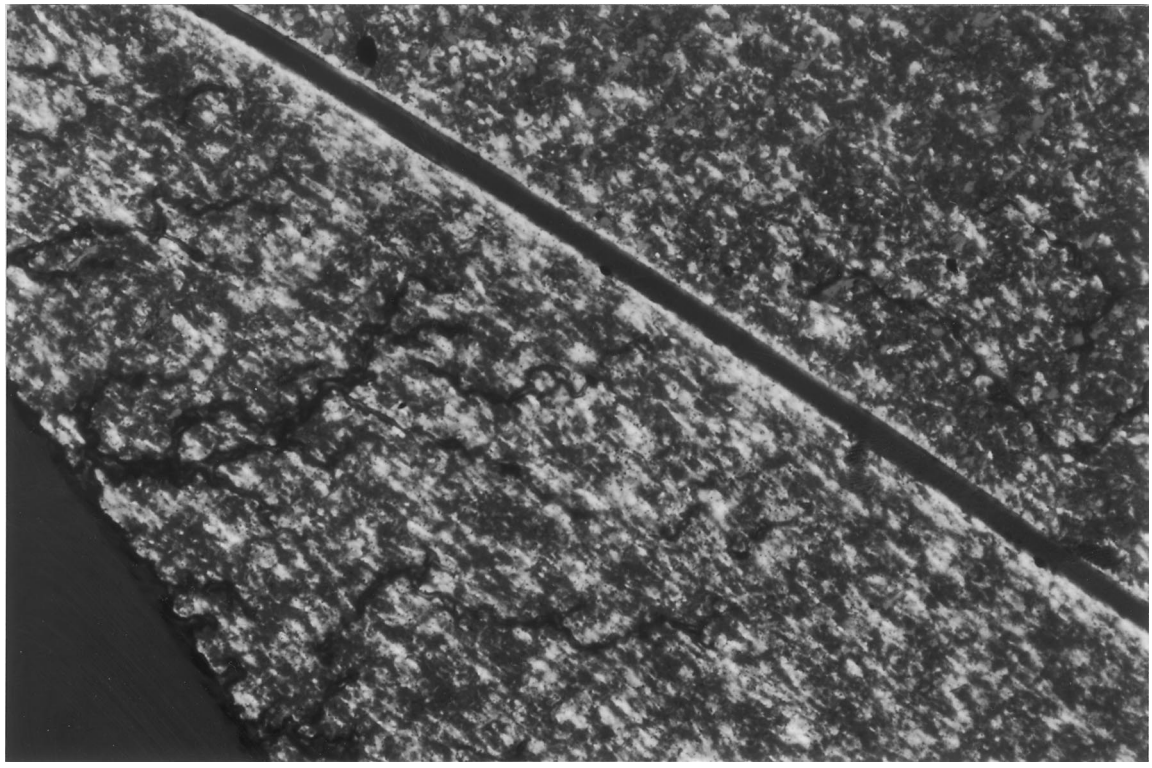

Figure 7 Polarised optical image of GF/PA6 thin film (cooling rate: $-3\,^{\circ}$C/min, holding pressure: atmosphere, magnification: $\times 250$).

the glass fibres. The pressure was found to be a very important parameter for the thermal processing of the thermoplastic composites. To break the surface energy of the nylon bubbles, a pressure was needed to force the matrix to wet the glass fibres. Without pressure voids form in the final products as shown in Figs 6 and 7. The GF/PA6 films were heated to molten state and then cooled down at 1 and 3 °C/min in the atmospheric pressure.

3. Experimental technique

Polyamide 6 is a semi-crystalline thermoplastic polymer. There is always an amorphous phase existing

in the bulk composite [20]. To obtain information regarding the crystallinity and crystal structures of the bulk GF/PA6 composites which were subjected to the three different cooling conditions, Differential Scanning Calorimetry (DSC) and X-ray Diffraction (XRD) measurements were performed in this study.

The different interfacial microstructures of the GF/PA6 thin films subjected to the different cooling rates were revealed by transmitted polarised optical microscopy using the Laborlux POL-12 optical microscope. The polarised images were taken by a Wild MPS 12 camera with magnification of $\times 250$.

Transmission Electron Microscopy was used to study the microstructures of nylon6 spherulites. The TEM samples were made from the above GF/PA6 films. The nylon6 spherulites of the thin films were examined by transmission electron microscope (Philips CM12) and operated at 120 kV. Philips EM 400 transmission electron microscope and EM430 electron energy loss spectroscopy (EELS), operating at 300 kV, were used to determine the nucleating agents in the nylon6 matrix.

3.1. Differential scanning calorimetry examination

The DSC test was carried out on a Mettler TA 4000 thermal analysis system with a heating rate of 10 °C/min. The average weight of the GF/PA6 samples for DSC test was 10 mg cut from the bulk composite and sealed in an aluminium shell. Both the melting point and percent crystallinity may be determined from a single DSC scan on the sample.

To calculate the percentage of crystallinity in the PA6 matrix, it is necessary to know exactly how much PA6 was in the GF/PA6 composite of the DSC sample. After DSC analysis, the GF/PA6 sample with a weight W_C was heated to 500 °C in an oven for 6 h burning the PA6 away. The sample remains were weighed on an analytical balance (sensitivity 0.01 mg) in the same atmosphere to determine the weight of the glass fibre (W_G). The percentage of the crystallinity of the GF/PA6 was calculated from the following expression.

$$\%\,\text{crystallinity} = (\Delta H_f/\Delta H_s) \times 100$$

where ΔH_s is 190 J/g, specific fusion endotherm of 1 g PA6 fully crystallised (Service instructions, Mettler TA-4000 manual, Version 6.7, 1990), ΔH_f is the measured heat of fusion endotherm of 1 g PA6 in the DSC sample and

$$\Delta H_f = H_f/(W_C - W_G)$$

H_f the peak area which was the heat of fusion or the fusion endotherm of the crystalline structure of the PA6 in the sample.

3.2. X-ray diffraction examination

The XRD method allows calculation of the relative amounts of crystalline and amorphous material in a sample provided that the contributions of the two types of structure to the X-ray diffraction pattern can be resolved. The estimation of the amount of crystallinity is usually based on a comparison of the areas under the peaks. With proper attention to experimental detail, this method provides a reliable measure of crystallinity in polymers [21, 22].

The XRD test was carried out on a Diffraktometer Siemens D5000 system. The sample was 50 mm in diameter and 4 mm in thickness which was cut off from the bulk GF/PA6 composites. One millimeter divergence slits and anti-scatter slits, a 0.2 mm receiving slit and a 0.6 mm detector slit were selected in this study.

In this test, the speed of the detector scanning step was 0.040°/30 s, low-angle X-ray diffraction ($2\theta = 10$ to 40 °C) and 60 rpm rotation were utilised. The sample was scanned for 6 h 16 min and 30 s.

4. Results and discussion

The test results of the DSC and XRD showed that the microstructures of the GF/PA6 composites were dramatically affected by the changing cooling rate. Slow cooling resulted in a high crystallinity and more α phase formed than the fast cooling process. The lamellae thickness was slightly affected by the cooling rate as well.

The details of the test results will be presented and discussed in detail in the following four parts; melting point, crystallinity, crystal phases and lamellae thickness.

4.1. Melting point

Figs 8–10 show the DSC results of the bulk GF/PA6 samples cooled down at different rates, respectively. The y-axis displays the endotherm (heat energy absorption by the crystalline PA6), the x-axis displays the temperature increasing in the DSC test. For the slowest cooling process (cooled down with hot-press, cooling rate: -1 °C/min) samples, the melting point was taken at the peak temperature, 226 °C, where the melting was virtually complete.

The peak area was equal to H_f which was the heat of fusion or the fusion endotherm of the α phase crystalline structures in the PA6 matrix of the GF/PA6 composite. Fig. 9 illustrates that there were two peaks appearing in the second slow cooled (cooled in air, cooling rate: -3 °C/min) GF/PA6 composite samples. The maximum trough within the shaded area represents the α phase, with $T_m = 226$ °C, and the inflection represents the γ phase, with $T_m = 220$ °C. However, the inflection disappeared in Fig. 10 which is the fastest cooling process (cooled in water, cooling rate: -60 °C/min) samples. On the chart (see Fig. 10), only the α phase appeared and it can be seen that its melting point is 226 °C. There should be γ phase present in the fastest cooled samples as XRD results indicate (see Fig. 11). However, this was not present in the DSC results because the $+10$ °C/min test heating rate in the DSC test converted the γ phase into α phase.

The difference between the melting points of the first two samples, -1 and -3 °C/min, indicated that

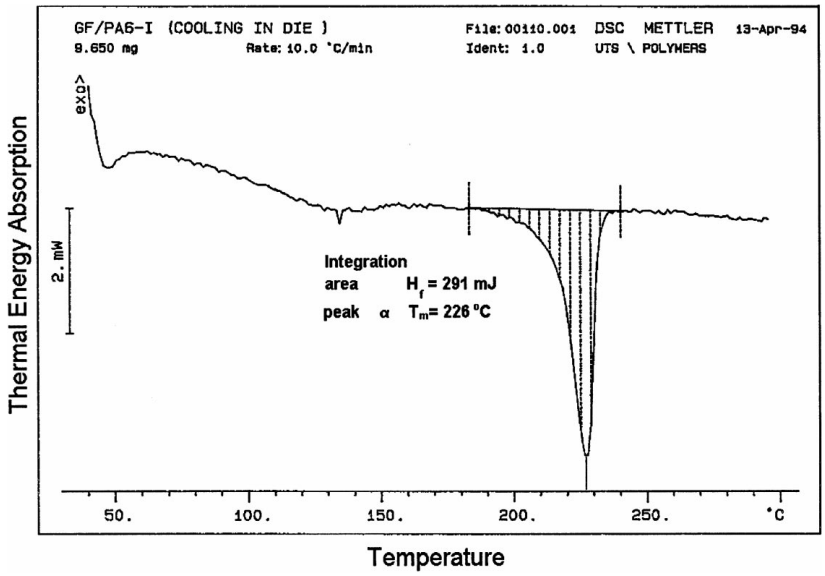

Figure 8 DSC heat flowing chart of GF/PA6 composite (cooling rate 1 °C/min).

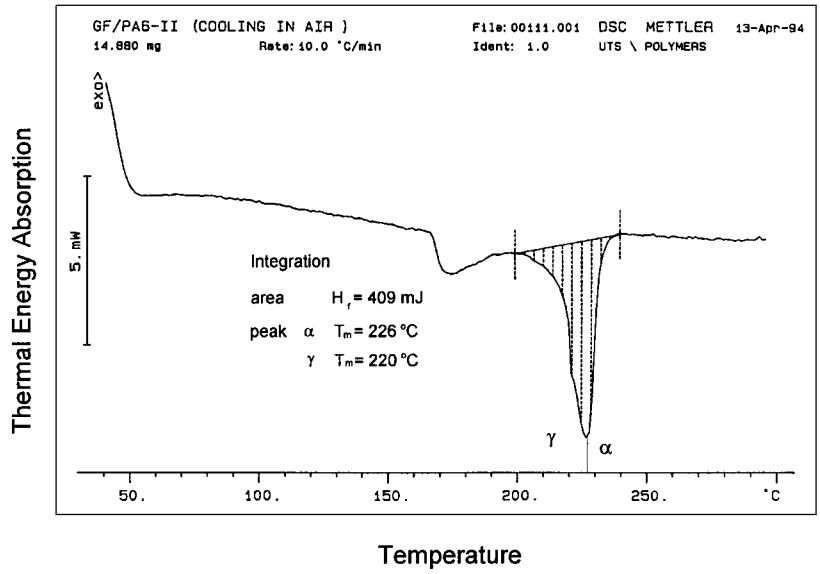

Figure 9 DSC heat flowing chart of GF/PA6 composite (cooling rate −3 °C/min).

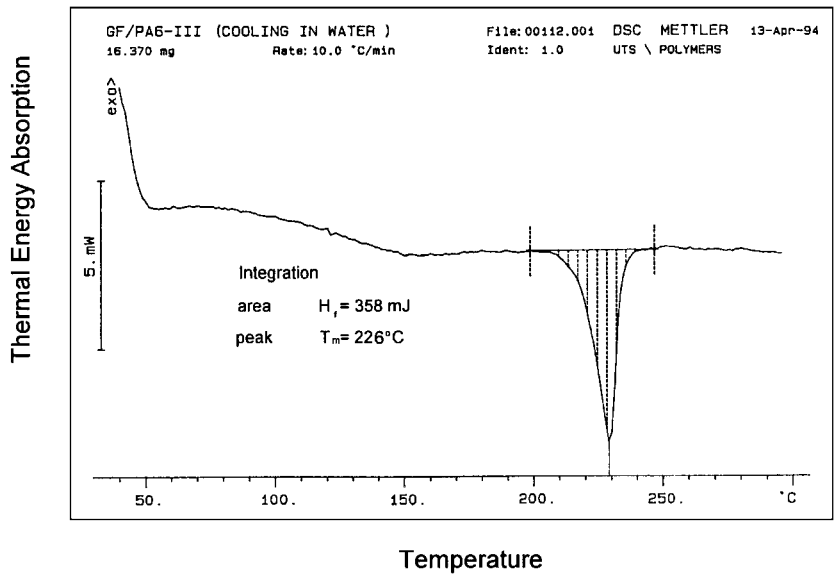

Figure 10 DSC heat flowing chart of GF/PA6 composite (cooling rate −60 °C/min).

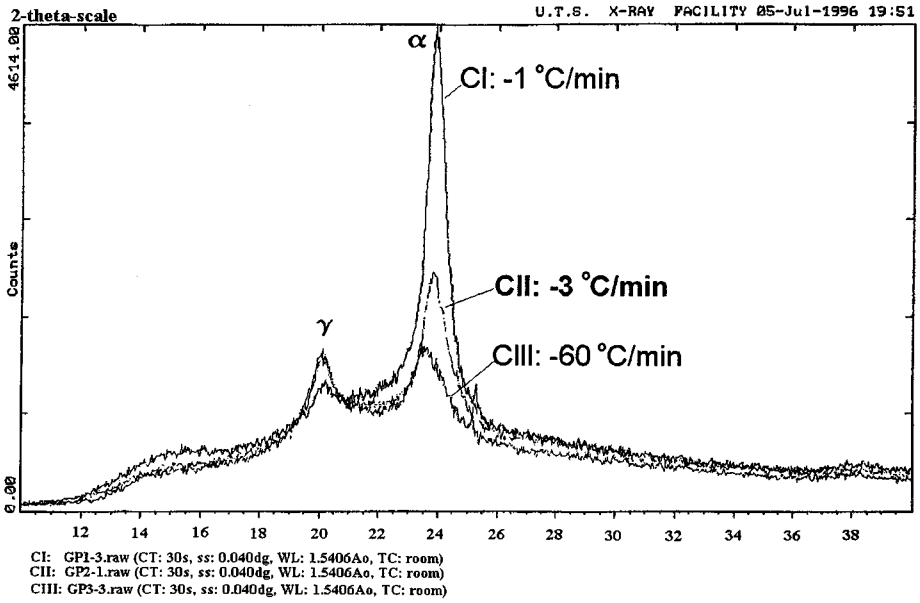

Figure 11 XRD diagram of GF/PA6 subjected to three different cooling rates.

decreasing the cooling rate in the thermal history increased the content of α phase crystal structures in the PA6 matrix. As shown in the DSC results, the α phase was associated with a high melting point and will result in the composites having a higher service temperature than that of γ phase samples which were formed in faster cooling processes.

4.2. Crystallinity

The results of the DSC analysis indicated that the crystallinity in the PA6 matrix of the unidirectional GF/PA6 bulk composite samples which were subjected to the three different cooling processes was dependent on the cooling rates. There were clear differences of crystallinity between the three GF/PA6 samples. Cooling with the hot-press ($-1\,^{\circ}$C/min) resulted in the highest crystallinity (X_c) at about 37%, followed by cooling with air circled ($-3\,^{\circ}$C/min) in the hot-press of 33% and water circled ($-60\,^{\circ}$C/min) in the hot-press resulted in crystallinity of 28% as shown in Table I.

Comparing the two Figs 8 and 10, it can be seen that the endothermic curve of the fastest cooled sample was similar as the curve of the slowest cooled sample. This is because the microstructures of the fast cooled samples had been changed during the DSC test. There was a re-crystallisation occurring during the DSC test due to its slow heating rate, $+10\,^{\circ}$C/min. Thus the DSC results of the fastest cooled samples, crystallinity may be higher than what they should be.

Due to the fact that the slow heating rate ($-10\,^{\circ}$C/min) in the DSC test was slower than the fast cooling rate ($-60\,^{\circ}$C/min) of the water cooled GF/PA6 samples, there could be more crystalline structures formed during the DSC test. It was similar to an annealing process during the slow heating in the DSC tests. Thus, the quantities of the CIII sample crystalline measured in the DSC test was higher than that of the water cooled original samples. The same situation may have occurred in the air cooled samples as well, as the DSC heating rate ($+10\,^{\circ}$C/min) was so close to the manufacture cooling rate ($-3\,^{\circ}$C/min). Therefore, it is necessary to check the crystallinity of the GF/PA6 by XRD method which does not involve heat and re-crystallization processes.

TABLE I The crystallinity of GF/PA6 composites from DSC test

Manufacture cooling rate	DSC test heating rate (°C/min)	Crystallinity of PA6 (%)
CI: $-1\,^{\circ}$C/min, hot-press	10	37
CII: $-3\,^{\circ}$C/min, air	10	33
CIII: $-60\,^{\circ}$C/min, water	10	28

The XRD test results indicated that the crystallinity and the α, γ phases contents of the three different cooling processing samples were significantly different under the same XRD testing condition. Fig. 11 shows the clear different intensities between the three cooling processes, the GF/PA6 bulk samples in the XRD test. The shaded area under the peaks present the crystalline volume [21, 22]. The first peak from the right hand side represents α phase and the second peak represents γ phase. The total shaded peaks area, α plus γ, implies the proportion to the total volume of the crystalline materials. The proportion of the peak areas of the three cooling rates samples was CI : CII : CIII $= 131.72 : 73.56 : 60.8 = 1 : 0.56 : 0.46$. Assuming the DSC result of crystallinity of the hot-press cooled sample (37%) was reliable and not affected by the heating rate in the DSC test, the crystallinity of air and water cooled samples can be calculated based on the proportion of the XRD results. The crystallinity results of the air and water cooled GF/PA6 composites were 20 and 17%, respectively. Table II lists the proportional relationship between peak area and the crystallinity of the nylon6 matrix in the GF/PA6 composites.

The XRD results verified that the crystallinity of the GF/PA6 samples cooled in the air and water evaluated during the DSC test due to its $10\,^{\circ}$C/min heating rate caused more crystal structures formed during the DSC

TABLE II The crystallinity of the GF/PA6 composites and peak area of the intensity in the XRD tests

Samples' cooling rate	$(\alpha+\gamma)$ peak area	Ratio of α/γ	X_c of PA6 (%)
CI: $-1\,^\circ$C/min, (hot-press)	$127+4.72=131.72$	27	37
CII: $-3\,^\circ$C/min, (air)	$52.94+20.62=73.56$	2.6	20
CIII: $-60\,^\circ$C/min, (water)	$33.61+27.19=60.8$	1.2	17

test. Thus, the DSC results of air and water cooled samples were not accurate.

From Table II, it can be seen that the crystallinity of the air cooled samples was quite close to the water cooled samples. This may probably be attributed to the crystalline forming speed of the nylon6 was very fast. A previous study [23] showed that it only takes 5 s for nylon6 to achieve half its potential crystallinity at the fastest crystalline temperature 140 °C. When the cooling rates are faster than $-3\,^\circ$C/min, the different cooling rates would not make much difference to the crystallinity. Based on the study of the thermal processing-crystallinity of the GF/PA6 and other references [20, 24], an attempt to produce a time-temperature-transformation diagram of the amorphous-crystalline phase changes during processing. Based upon the XRD data, Fig. 12 illustrates such an approximate for the nylon6 in this study. The glass transition temperature is 50 °C [25], the fastest crystal growth temperature is 140 °C and the melting point is 240 °C, respectively, in the TTT plot.

4.3. Crystal phases

From the DSC study of the GF/PA6 composites, it has been found that two phases α and γ existed in the nylon6 matrix and this has been verified by the XRD test results. In Fig. 11, it can be seen that there are two peaks appearing in all of the three cooling rate samples. The Bragg's angle θ of the first peak which is from the right hand side is over 23°. The second peak falls between 20 and 23°. The two peaks represent the α and γ phases in the crystal structures of the nylon6 matrix. Also it can been seen that there are amorphous phases in the background.

The XRD results showed that decreasing the cooling rate during moulding led to more α crystal structures formed than γ phase in the nylon6 matrix. The CI samples have extremely higher contents of the α phase than that of CII and CIII samples. It also can be seen from Fig. 11, that CII and CIII samples have the same volume of γ phase content. The γ phase content of CI sample is less than that of CII and CIII samples. Table II lists the different ratios of the α and γ phases in the PA6 matrix due to the three different cooling processes.

It has been reported that the hydrogen bonding angle of the α crystal is larger than that of γ crystal, thus the α chain is straighter and longer than that of the γ chain. The distance between adjacent chains in α crystal is shorter than that of the γ phase, thus the chains are packed tighter in α crystal than the γ crystal [18, 26]. Therefore, the density of α crystalline materials is higher than that of γ materials. Consequently, the hardness and Youngs modulus of α phase may be higher than that of γ phase.

There is some interesting evidence from Murthy and Bray's recent research [15] verifying the above assumption. Nylon6 specimens with a higher content of the α phase have higher density (1.24 g/cm^3), crystalline perfection, T_g, tensile strength and modulus than that of γ phase (1.17 g/cm^3). Their infrared spectroscopy and X-ray diffraction studies showed that to separate the γ phase and the amorphous scattering is very difficult when the γ phase is either poorly formed and/or is very low. The IR spectra of the γ phase and the amorphous are very similar to each other and very different from that of the α phase. This is because of the γ chain and the amorphous chain possess very similar conformations. Murthy also found that T_g increased with increasing

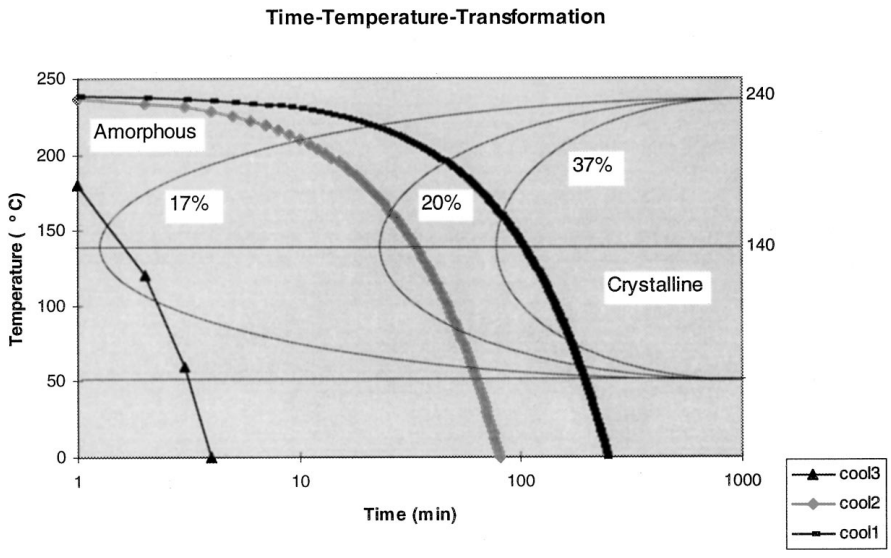

Figure 12 Amorphous-Crystalline transformation in nylon6: an assumed diagram of Time-Temperature-Transformation (The cool1 curve represents the cooling rate 1 °C/min, cool2 is 3 °C/min and cool3 is 60 °C/min, respectively).

proportions of α phase. Increasing T_g can result in low-wear materials in tribological applications [27].

The α phase has a higher thermodynamically stable structure than the γ phase. The heat of fusion of α phase (241 J/g) was found to be higher than the γ phase (239 J/g) [28]. The peak of mechanical loss, tan δ, decreases with an increasing α phase crystallinity [29]. These characteristics of the α phase may give the composites a higher service temperature than that of γ phase.

The purpose of determining the various structural parameters described here is to be able to predict the properties and performance of the GF/PA6 composites. One of the most obvious differences that stands out in examining the X-ray scans of any sample was the relative amounts of the α and γ crystallinities. This α/γ ratio was quite useful because it reflected the manufacturing history of the GF/PA6 composites. The parameters that are likely to be directly useful in predicting the properties are the total crystallinity and the orientation of the matrix. The α and γ contents have significant influence on the mechanical, interfacial and wear properties of the composites which were presented separately in other papers [30].

4.4. Lamellae thickness

From molten state to solid some nylon6 chains are folded and packed orderly together forming a thin and flat platelets (lamellae crystal) about 100 Å thick and 1000 Å to 1 μm in lateral dimensions. The thickness of the lamellae depends on many factors during the thermal processing such as crystallization temperature, pressure and holding time. For example, the specific temperature of the fastest growth of the nylon6 lamellae or spherulite is 140 °C [31]. If the sample is cooled slowly from molten state, it will stay in the specific temperature longer than that for the fast cooled sample. Thus, there will be thicker lamellae or large spherulite found in the slow cooled samples than that of fast cooled samples as Fig. 11 shows. It can be seen in the Fig. 11 that the full width at half peak height of α phase is slightly narrower in the CI sample than that of CII and CIII samples.

The XRD results indicated that the full width at the half peak maximum intensity (FWHM) of the α phase in the three different cooling processed samples are CI: 1.028°, CII: 1.132°, CIII: 1.335°, respectively. This means the lamellar thicknesses of the three different cooled samples were different. The thicknesses of the lamellar crystal in the three different cooled GF/PA6 composites can be calculated by using the Scherrer formula [32].

$$L_{lt} = K\lambda/(\beta_0 \cos\theta)$$

where L_{lt} is lamellar thickness in Å, $K = 0.9$, a constant that is commonly assigned a value of unity, $\lambda = 1.54059$ Å , X-rays wavelength, θ the Bragg's angle, and $\beta_0 =$ FWHM, the full width at half peak maximum intensity, the breadth of the reflection corrected for instrumental broadening in degree and should be converted by $\pi/180$

$$\beta_0 = \sqrt{\beta_m^2 - \beta_s^2}$$

where β_m is the measured peak width at half peak height and β_s the corresponding peak width of a standard material or breadth of instrumental broadening, for D5000 is silicon, 0.1°.

TABLE III XRD test results of the lamellar thickness of α crystallite in the nylon6 matrix of GF/PA6 composites subjected to three different cooling rates

Cooling condition	2θ	β_m, measured FWHM	α, lamellar thickness (Å)
CI: −1 °C/min hot-presscooled	23.891	1.0281°	79.36
CII: −3 °C/min air cooled	23.864	1.1322°	71.99
CIII: −60 °C/min water cooled	23.440	1.3346°	60.96

Table III lists the thickness of the α phase lamellar crystal in the GF/PA6 matrix which were subjected to the three different cooling processes. The results showed that cooling rate has slightly affected the lamellar thickness. Slow cooling gave the nylon6 thicker lamellar crystal than that of fast cooling process.

In general, the thickness of lamellae can affect the mechanical properties of polymers. Increasing lamellar thickness (spherulite size) will result in decreasing toughness and rupture elongation, and increasing tensile strength and modulus of the polymers [33].

4.5. Interface

The Polarised Optical Microscopy (POM) study of the GF/PA6 thin films showed that there was columnar spherulitic growth along the glass fibre in the slowest cooled samples. It may be a transcrystalline region between the matrix and fibre. The columnar spherulite structures disappeared with increasing cooling rate in the samples. Figs 13–15 show the microstructures of the glass fibre reinforced nylon6 subjected to the three different cooling conditions. It can be seen in Fig. 13, the hot-press cooled sample, that there was a columnar spherulite structure in between of the glass fibre and nylon6 matrix. The columnar spherulite structure may be a transcrystalline layer. The diameter of the columnar spherulite was affected by the cooling rate. A slow cooling process led to a larger diameter of the columnar spherulites than the fast cooling process. The columnar spherulite structure disappeared in the fast cooled film samples as shown in Fig. 15, and there are two clear border lines between the glass fibre and matrix. It seems the interfacial bond between the glass fibre and nylon6 matrix was very poor in the water cooled samples.

Additionally, the pressure has affected the interfacial bond as well. Cracks were found between the glass fibre and nylon matrix in the hot-press cooled samples without applied holding pressure as shown in Fig. 6. In

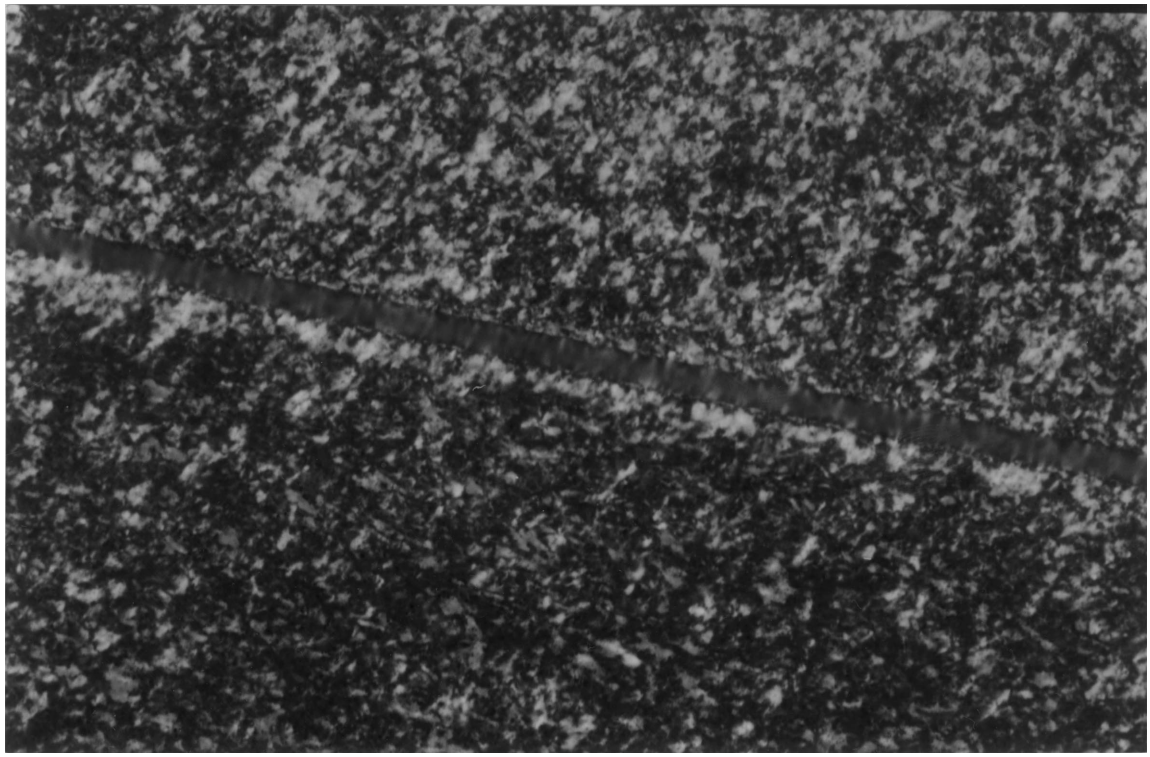

Figure 13 Polarised optical image of GF/PA6 thin film cooled in hot-press (cooling rate:- $-1\,^{\circ}$C/min, holding pressure: 1.5 MPa, magnification: $\times 250$).

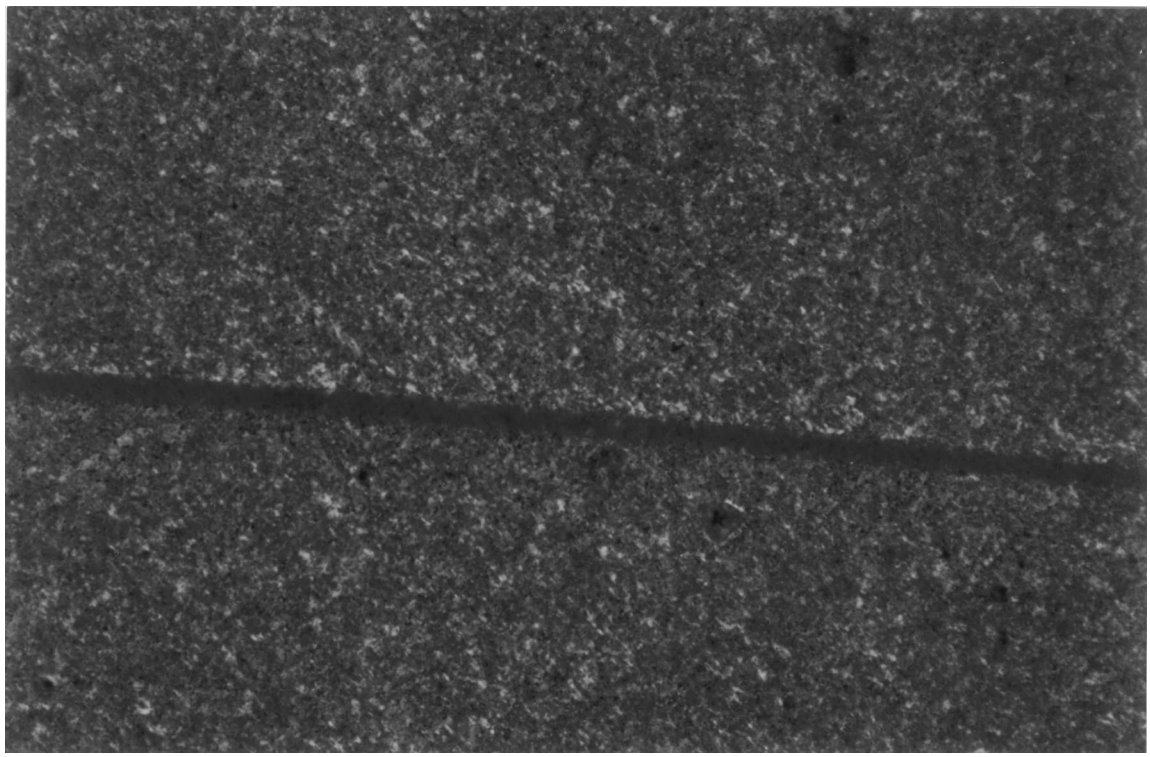

Figure 14 Polarised optical image of GF/PA6 thin film cooled with air circling in hot-press (cooling rate: $-3\,^{\circ}$C/min, holding pressure: 1.5 MPa, magnification: $\times 250$).

Fig. 13, it can be seen that there was good interfacial bond in the GF/PA6 sample which was cooled in the hot-press with 1.5 MPa pressure.

From POM observation of both the GF/PA6 samples, it can be concluded that the cooling rate has significantly affected the transcrystallinity. Decreasing cooling rate may increase the transcrystallinity (the thickness of the transcrystalline layer). The interfacial bond was influenced by the holding pressure as well. Low holding pressure during thermal processes also led to a poor interfacial bond in the thermoplastic composites (see Fig. 6).

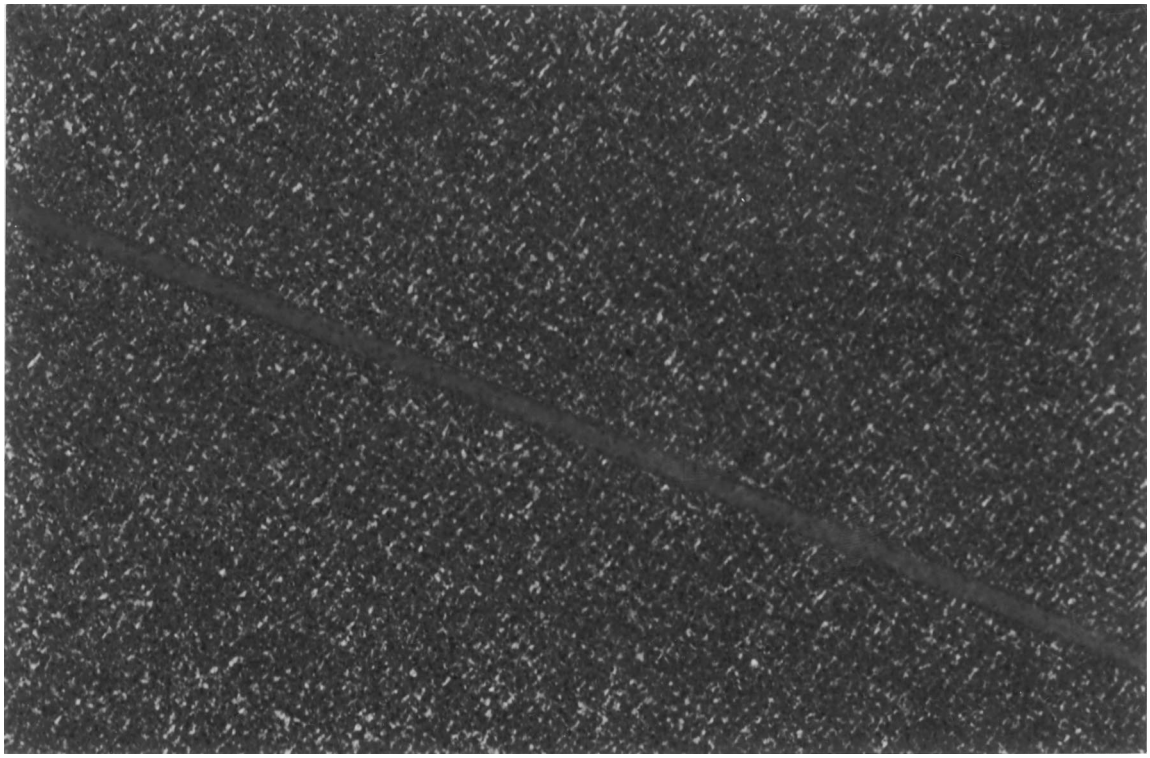

Figure 15 Polarised optical image of GF/PA6 thin film cooled with water circling in hot-press (cooling rate: $-60\,^{\circ}$C/min, holding pressure: 1.5 MPa, magnification: $\times 250$).

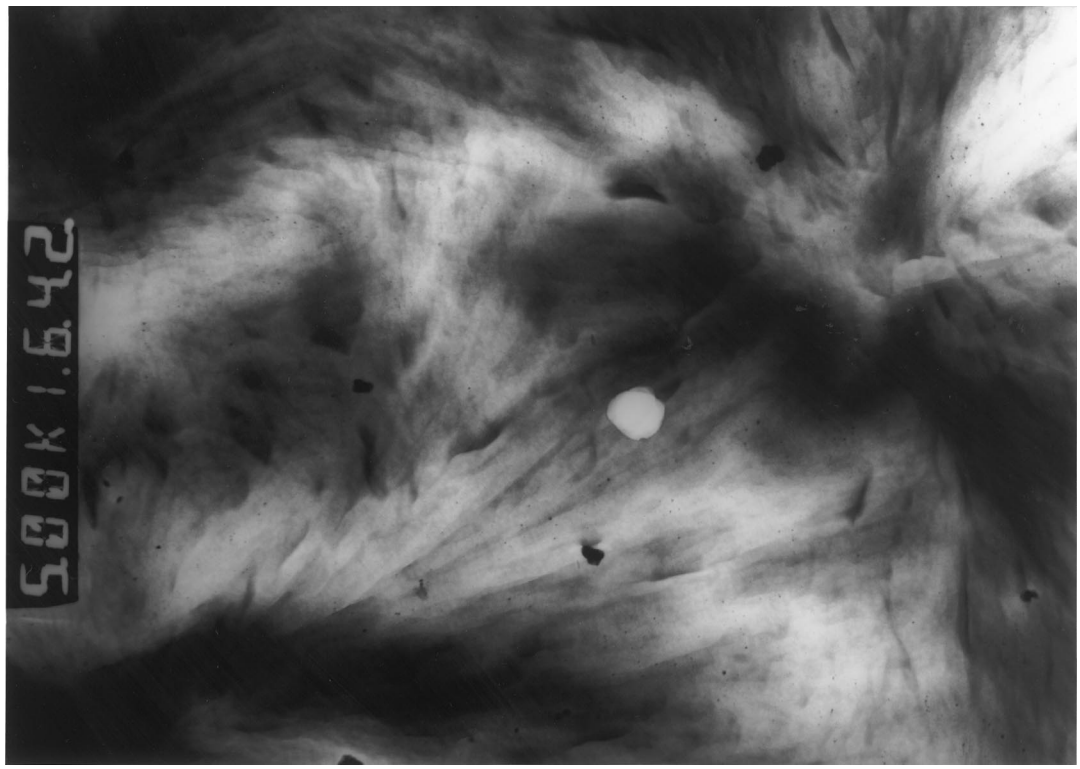

Figure 16 TEM photograph of nylon6 spherulites cooled in hot-press with atmospheric pressure (magnification: $\times 9500$).

4.6. Spherulite

It was also found in the polarised images, Figs 13–15 of the GF/PA6 films, that the spherulite size of the PA6 matrix was affected by the cooling rates. Decreasing cooling rate may result in larger size spherulites. This result is consistent with the XRD results of bulk GF/PA6 samples which was presented in Section 4.4, Table III.

It has been reported that the spherulite size can affect the short term mechanical properties of the semicrystalline polymers. An increased spherulite size and crystallinity normally results in increased tensile strength and yield strength, but lower rupture elongation and toughness [33]. Also under long term stress conditions, in either cyclic/fatigue or static/creep loadings, slow

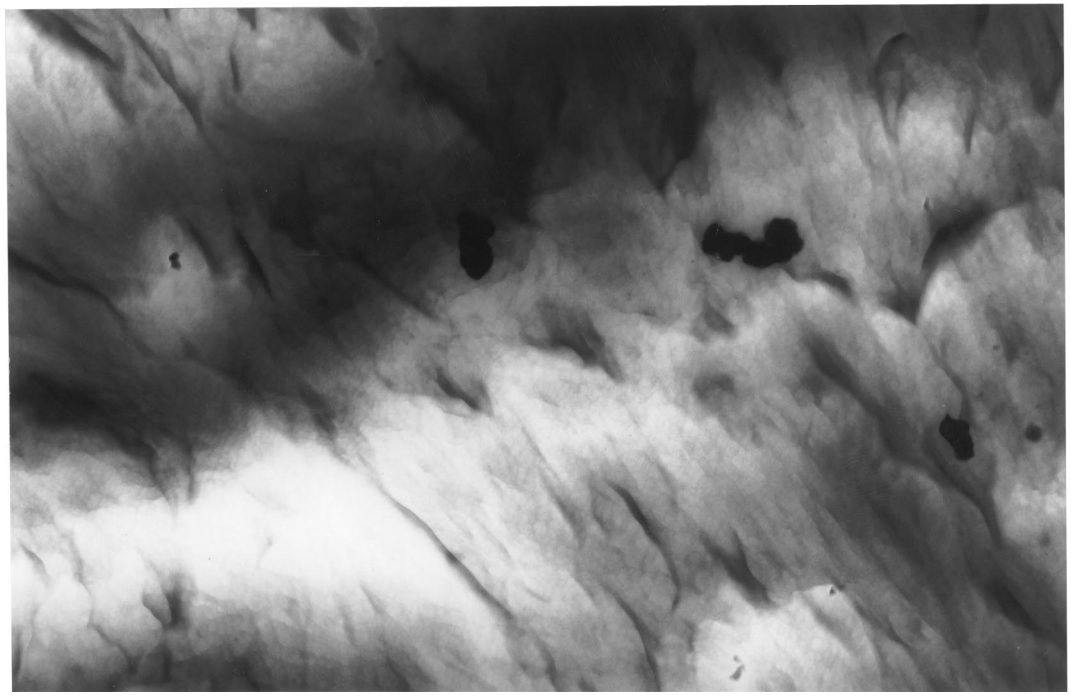

Figure 17 TEM photograph of nylon6 spherulites cooled in hot-press with atmospheric pressure (magnification: ×16000).

stable cracks are found to form in polyethylene at the boundaries of spherulites and within them. Lustiger suggested that the primary long term failure mechanism in these materials is separation between lamellae [34].

The microstructures of the nylon6 spherulite has clearly been revealed by the TEM technique images (Figs 16 and 17). It can be seen that the lamellae grow from the centre of the spherulite and smoothly join into adjacent spherulites. It was hard to distinguish the boundary between the spherulites. Normally the spherulites boundary is the weakest area of the material. If the boundary joint is smooth and not clearly defined that might result in strong materials.

5. Conclusions

Through the microstructure study of the GF/PA6 composites subjected to the different cooling rates during thermal manufacturing, the following conclusions can be drawn.

(1) The microstructures of the GF/PA6 bulk composites were significantly affected by the different thermal processes. The results of the DSC and XRD tests showed that slow cooling process led to a higher crystallinity and higher ratio of the α to γ phases in the nylon6 matrix than that of fast cooling process.

(2) The DSC results showed that the melting point of the α and γ phases of the nylon6 in the GF/PA6 composites was 226 and 220 °C, respectively.

(3) The XRD results also indicated that the lamellae thickness of the nylon6 was slightly affected by the cooling rate. The slow cooling led to thicker lamellae formed during the thermal processing than that of fast cooling process.

(4) Microstructure study of the GF/PA6 thin films showed that columnar spherulites grew along the glass fibres which may be transcrystalline layers. The columnar spherulites disappeared with increasing cooling rate.

(5) The different thickness of the transcrystalline layers were found to be influenced by the different cooling rate. Slow cooling led to a larger diameter of the columnar spherulites than the fast cooling process. The POM results also showed that slow cooling led to larger size spherulites in the nylon6 matrix than the fast cooling process.

(6) Microscopy study of the thermal processing GF/PA6 on the hot-stage showed that the holding pressure was a important parameter in the thermal processes. Sample consolidated without holding pressure resulted in large voids and poor interfacial bond in the composites.

Acknowledgements

The authors would like to give their special thanks to Professor Mike Swain who is from Mechanical and Mechatronic Engineering Department of Sydney University for the many long and valuable discussions through out this study. The authors would also like to thank Professor Bob Cheery at the University of Technology, Sydney, for his many useful discussions of the XRD results. The authors would like to acknowledge the Australian Postgraduate Research Award for the financial support given to Dr. Helen Cartledge throughout this study and the Toyobo Research Institute, Japan, for providing the GF/PA6 commingled yarn materials used in this study.

References

1. J. SEFERIS, *Polymer Composites* **7**(3) (1986) 158–169.
2. W. LEE, M. TALBOTT, G. SPRINGER and L. BERGLUND, *J. Reinforced Plastics and Composites* **6**(1) (1987) 2–12.

3. P. DAVIES, W. CANTWELL, P. JAR, H. RICHARD, D. NEVILLE and H. KAUSCH, Cooling Rate Effects in Carbon Fibre/PEEK Composites, Composite Materials: Fatigue and Fracture, ASTM STP 1110 (American Society for Testing and Materials, Philadelphia, 1991) 70–88.
4. H. LIN, R. LEE, C. LIU, J. WU and C. HUANG, *Composites Science and Technology* **52** (1994) 407–416.
5. P. CURTIS, P. DAVIES, I. K. PATRIDGE and J. P. SAINTY, "Cooling Rate Effects in PEEK and Carbon Fibre-PEEK Composites," Proceeding of ICCM6-ECCM2 (Elsevier Applied Science, London, 1987), pp. 4.401–4.412.
6. J. SEFERIS, C. AHLSTROM and S. H. DILLMAN, *ANTEC* (1987) 1467–1471.
7. S. SIELLO, J. KENNY and NICOLAIS, *J. Mater. Sci*. **25** (1990) 3493–3496.
8. M. KANTZ and R. D. CORNELIUSSEN, *J. Polym. Sci. Polym. Lett. Ed*. **11** (1973) 279.
9. F. COGSWELL, in Proceedings of the 28th National SAMPE Symposium, 1983, pp. 528–534.
10. Y. LEE and R. S. PORTER, *Polym. Eng. Sci.* **26** (1986) 633.
11. M. MATSUO, R. SATO and Y. SHIMIZU, *Colloid & Polymer Science* **271**(1) (1993) 11–21.
12. D. PREVORSEK and H. B. CHIN, *Int. J. Polym. Mater* **25** (3/4) (1994) 161–184.
13. M. EVSTATIEV and M. SARKISOVA, *Vysokomolekulyarnye soedineniya seriya A* **37**(2) (1995) 237–241.
14. D. HOLMES, C. W. BUNN and D. J. SMITH, *J. Polym. Sci*. **17** (1955) 159–177.
15. N. MURTHY and R. G. BRAY, *Polymer* **36**(20) (1995) 3863–3873.
16. M. KOHAN, "Nylon Plastics" (John Wiley & Sons, New York, 1973).
17. Y. KINOSHITA, *Makromol. Chem*. **33** (1959) 1.
18. H. ARIMOTO, *J. Polym. Sci. A* **2** (1964) 2283–2295.
19. H. ARIMOTO, M. ISHIBASHI, M. HIRAI and Y. CHATANI, *J. Polym. Sci. A* **3** (1965) 317–326.
20. M. ASHBY and DAVID R. H. JONES, "An Introduction to Microstructures, Processing and Design," International Series on Materials Science and Technology, Vol. 39, 1992.
20. M. ASHBY and D. JONES, *Eng. Mater*. **2** (1992) 72–73.
21. F. BILLMEYER, JR., "Textbook of Polymer Science" (John Wiley & Sons, New York, 1984).
22. L. ALEXANDER, "X-ray Diffraction Methods in Polymers Science" (New York, John Wiley & Sons, 1969).
23. ZHONG *et al.*, 1981.
24. R. YOUNG, "Introduction to Polymers," 1983, pp. 184–193.
25. ARVANITOYANNS and PSOMIADOU, 1994.
26. G. HATFIELD, J. H. GLANS and W. B. HAMMOND, *Macromolecules* **23** (1990) 1654–1658.
27. J. YOO and N. S. EISS, JR., *Wear* **162–164** (1993) 418–425.
28. K. ILLERS, *Makromol. Chem*. **179** (1978) 519.
29. N. MCCRUM, "Anelastic and Dielectric Effects in Polymeric Solids" (John Wiley & Sons, London, 1967) p. 478.
30. H. CARTLEDGE and C. A. BAILLIE, *J. Mater. Sci*. **34** (1999) 5113.
31. P. HENDRA, "Structural Studies of Macromolecules by Spectroscopic Methods," chap. 6, edited by K. Ivin (John Wiley & Sons, New York, 1979).
32. P. SCHERRER, *Gottinger Nachrichten* **2** (1918)98.
33. A. LUSTIGER, *SAMPE J*. **20** (5) (1984) 13.
34. A. LUSTIGER, *Polymer*, **24** (1983) 1647.
35. Z. XIU *et al*., "The Structures and Properties of Polymers" (Science Publisher, Beijing, China, 1981) p. 115.

Received 5 February 1998
and accepted 8 February 1999